Direct conversion of CO2 and CH4 into liquid chemicals by plasma-catalysis

Di Li, Vandad Rohani, Frédéric Fabry, Aravind Parakkulam Ramaswamy, Mohamed Sennour, Laurent Fulcheri

To cite this version:

Di Li, Vandad Rohani, Frédéric Fabry, Aravind Parakkulam Ramaswamy, Mohamed Sennour, et al.. Direct conversion of CO2 and CH4 into liquid chemicals by plasma-catalysis. Applied Catalysis B: Environmental, 2020, 261, pp.118228. 10.1016/j.apcatb.2019.118228 . hal-02886661

HAL Id: hal-02886661
https://minesparis-psl.hal.science/hal-02886661

Submitted on 20 Jul 2022

Direct conversion of CO_2 and CH_4 into liquid chemicals by plasma-catalysis

Di Li[1], Vandad Rohani[1,*], Frédéric Fabry[1], Aravind Parakkulam Ramaswamy[1], Mohamed Sennour[2], Laurent Fulcheri[1]

1. PSL Research University, MINES ParisTech, PERSEE - Centre Procédés, Énergies renouvelables et Systèmes énergétiques, 1 Rue Claude Daunesse, 06904 Sophia Antipolis, France

2. PSL Research University, MINES ParisTech, Centre des Matériaux, 63-65 rue Henri Auguste Desbruères - B.P. 87 à côté de SNECMA, 91003 Evry Cedex, France

Abstract: A plasma-catalytic reactor consisting in a vertical coaxial dielectric barrier discharge reactor filled with solid catalysts was developed to directly synthesize liquid chemicals (alcohols, acids, hydrocarbons) and syngas from CO_2 and CH_4 at atmospheric conditions. Co and Fe catalysts prepared via incipient wetness impregnation method were loaded on a SiO_2 aerogel support synthesized by ambient drying method after surface modification. Discharges were generated in different ratios of CO_2/CH_4 mixtures at ambient conditions and the performance of the catalysts was evaluated. In this study, the total liquid selectivity was approximately 40% after introducing the catalysts, where main liquid products were methanol and acetic acid. By varying the CH_4 and CO_2 ratio, a small number of long-chain hydrocarbons and alcohols were also detected with our catalysts. The synergy of plasma-catalysis in this process demonstrates great potential for the direct synthesis of value-added liquid chemicals and fuels from CO_2 and CH_4.

Keywords: hydrocarbon synthesis, non-thermal plasma, liquid products, catalysts

1. Introduction

In recent centuries, the accumulation of greenhouse gases such as CO_2 and CH_4, has contributed to climate change due to excessive emissions from fuel combustion, refinery plants, petrol industries, chemical industries, etc. Many techniques have been proposed to reduce the concentration of greenhouse gases as well as utilization, among those CO_2 capture has been regarded as an efficient one and is progressively applied in chemical and energy industries. However, storage of CO_2 still has significant issues regarding the high investment, transportation, and uncertainty of long-term storage [1]. Under this context, indirect and direct chemical conversion of CO_2 with CH_4 into value-added chemicals has attracted great attention and interest for its potential to achieve a sustainable and low carbon emission process in chemical and oil refinery industries and avoid the inconvenience of storage [2, 3]. For the indirect approach, which has been researched for decades, CO_2 and CH_4 mixture is first converted into syngas products. Then the syngas can be transformed into liquid fuels and other oxygenated chemicals by FTS process. For the more interesting direct approach, it is still a great challenge to us.

The thermodynamic stability of the CO_2 molecule is well known. The activation of CO_2 generally requires significant energy consumption, which makes the efficient activation and conversion of CO_2 a great challenge. Some researchers have focused their efforts on studying conventional thermochemical methods, including dry reforming to syngas, and direct conversion to liquid organics, associated with various catalysts. However, the essential high temperature and the deactivation of catalysts are critical issues and drawbacks [4]. In recent decades, non-thermal plasma (NTP) has been exploited and applied to various fields, such as degradation of pollutants and synthesis of chemicals, as it offers a unique pathway to induce thermodynamically unfavorable chemical reactions at a low temperature due to its high concentration of energetic and chemically active species [5]. The typical electron temperature (1-10 eV) of NTP is sufficient to activate CO_2 (5.5 eV) and CH_4 (4.5 eV) molecules into reactive radicals, excited molecules, atoms, and ions, which are energetic enough to initiate chemical reactions between CO_2 and CH_4. Moreover, plasma discharge can be easily generated by applying voltage, where the renewables are holding more and more shares in power generation. Therefore, the whole process can achieve a low emission and offer an alternative way to store renewable energy.

Enormous efforts have been dedicated to exploring the plasma-catalytic conversion of CO_2 with CH_4, including studies on the effects of different plasma types, experimental variables and reactors to improve the conversion and selectivity to syngas products [6-17]. Moreover, various catalysts and packing materials have been investigated on plasma-catalytic reforming of CO_2 and CH_4, including zeolites and some metal catalysts with their supports [18-23]. Tu et al. [24, 25] reported that full packing of Ni/Al_2O_3 catalysts in the discharge volume could modify the discharge behavior from a typical filamentary discharge to a combination of surface discharges and spatially limited microdischarges, leading to a decrease of power in the discharge and conversion of reactants. Zou et al. [26] demonstrated the possibility that starch could directly enhance the oxygenate formation from methane and carbon dioxide. Scapinello et al. [27] explored the formation of carboxylic acids on the surface of copper and nickel electrodes. Other researchers also reported the formation of oxygenates as by-products in plasma-promoted reforming, although selectivity was still poor and external heating was essential [9, 28, 29]. Wang et al. [30] demonstrated the synthesis of a considerable production of liquid chemicals, including acetic acid, methanol, and acetone, via a novel DBD reactor equipped with a ground water electrode. They reported that the combination of a plasma process and Cu, Au, and Pt-Al_2O_3 showed potential for the direct production of oxygenates under ambient conditions. However, most works mainly focused on the dry reforming of CO_2 and CH_4 into syngas production. Although the formation of methanol or formic acid has been reported by photocatalytic reduction of CO_2 [31-33], few efforts have been dedicated to plasma-catalytic synthesizing liquid chemicals (including hydrocarbons) directly from CO_2 and CH_4 with a considerable selectivity under ambient condition.

Formerly, our group has worked on the hydrocarbon synthesis through arc discharge at high pressures [34, 35]. In this study, we developed a plasma-catalytic reactor consisting of a vertical coaxial DBD reactor packing with metal doped SiO_2 aerogel catalysts, for the direct synthesis of liquid chemicals at ambient conditions. The metal catalysts we used in this work are Co and Fe, which are widely used in CO_2 hydrogenation and FTS process due to their high activity to CO_2 activation and chain propagation. The highly porous hydrophobic SiO_2 aerogel support was designed and synthesized via ambient drying method after surface modification to avoid an extreme abatement in the discharge volume. The Co- and Fe-loaded SiO_2 aerogel catalysts were obtained by incipient wetness impregnation and then characterized. Finally, the catalysts were fully packed into the reactor, and the experimental study on catalytic performance was carried out and presented by comparing to no packing condition.

2. Methods and materials

2.1. Experimental setup

The schematic diagram of the setup is shown in Scheme 1. It was comprised of a power supply, a DBD reactor, a product collector, and an analysis system. The schematic diagram of the DBD reactor is presented in Scheme 2. The DBD reactor mainly included two coaxial electrodes and a dielectric ceramic tube. The inner high-voltage electrode was an aluminum rod with a diameter of 6 mm coaxially installed in the ceramic tube (10 mm i.d. × 12 mm o.d.); two evenly distributed adjustable Teflon caps (6 mm i.d. × 10 mm o.d.) with 12 semi-circle pores (1mm i.d.) were coupled with the aluminum rod to ensure the concentricity of the electrode in the ceramic tube and to fix the full-packed catalysts; the outer grounded electrode was a 200 mm-long stainless-steel coil wrapped around the dielectric tube. A compressed air gun was installed facing the reactor to avoid possible overheating; an IR camera (IRISYS IRI 4010) was used to measure and monitor the temperature of the reactor. The power supply system applied to the reactor was composed of a signal function generator (HP 33120A), an audio amplifier (IMG Stageline STA-1400) and a transformer. The amplifying output level range of the audio amplifier varies from “-80 dB” to “0 dB”, therefore the peak-to-peak voltage can be adjusted. Five different signals with a variable frequency can be generated through the function generator. In this work, the frequency of the sinusoidal signal was fixed at 3 kHz, and the peak-to-peak voltage was fixed at 5.5 kV. The Lissajous method was applied to calculate the applied power by connecting a capacitor (3.9 nF) in series with the reactor. Two high-voltage probes were applied to measure the voltage of the plasma reactor and the capacitor; two temperature probes were installed inside the reactor’s gas inlet and outlet respectively to measure the temperature of the inlet and outlet gas; one pressure probe was installed before the gas inlet to monitor the pressure of inlet gas. The real-time temperature and pressure data were monitored and recorded simultaneously on a computer via a Keysight 34970A Data Acquisition unit. The electrical data were monitored in real time via a digital oscilloscope (HP Hewlett Packard 54615B) and recorded by the computer separately. The data files were recorded by 1,000 points for each of 2 channels once.

The gaseous products were analyzed online by a micro gas chromatography (Micro GC Fusion) equipped with two channels (an Rt-Molsieve 5 Å, R 0.25mm, L 10m column and an Rt-Q-Bond, R 0.25mm, L12m column) and two thermal conductivity detectors (TCD). An icy water trap was used to condense the liquid products before the micro GC. The liquid products were analyzed offline using a gas chromatography-mass spectrometer (GCMS-QP2010, Shimadzu) equipped with a SUPEL-Q PLOT (R 0.32mm, L 30 m) column. The difference in gas volume before and after the discharge was measured at the outlet by a soap-film flowmeter.

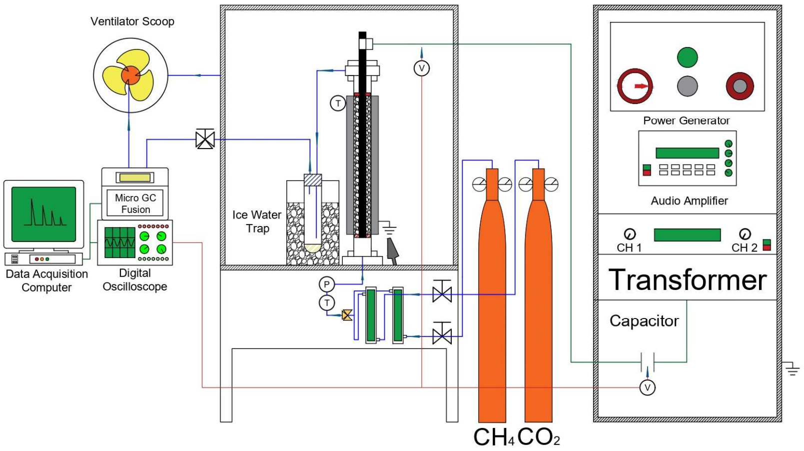

Scheme 1. Schematic diagram of the experimental setup.

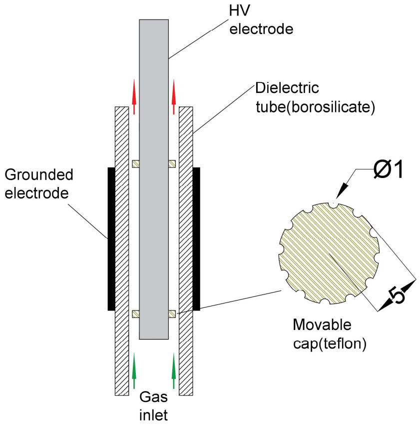

Scheme 2. Schematic diagram of the DBD reactor.

2.2. Materials and analysis

The silica aerogel support was prepared using polyethoxydisiloxane (P75W20, PCAS, <30%) as silica precursors via a sol-gel method. 10 g of P75W20 was added to 15 g of ethanol (Fisher Scientific, Absolute) in a polyethylene vial while stirring. The solution was kept for 5 mins, after which 2625 μL of distilled water was added to act as a hydrolysis agent, and 2955 μL of (3-Aminopropyl) triethoxysilane (APTES, Thermo Fisher, 98%) solution (APTES: Ethanol = 1:50) was added to adjust the pH value for gelation. The final mixture solution was covered and allowed to gel and age at 60 °C for 48 h. Following the aging, 35 mL of Hexamethyldisilazane (HMDZ, Acros Organics, 98%) was added to the silica gels and left covered for 3 nights at ambient conditions to remove the hydroxyl groups. In the next step, the hydrophobic silica gels were washed in ethanol 5 times (over 2 days) to remove excessive HMDZ. The final gels were then transferred into an oven and dried for 2h at 140 °C.

The Co/SiO_2 and Fe/SiO_2 aerogel catalysts with the targeted mass ratio of Co or Fe loading (10% metal to silica) were prepared by the incipient wetness impregnation method. The targeted ethanolic solution of $Fe(NO_3)_2{\cdot}9H_2O$ and $Co(NO_3)_2{\cdot}6H_2O$ (Acros Organics, ≥99%) was mixed with the same volume of silica aerogels prepared by the sol-gel method and maintained impregnated for one night. In the next step, the samples were dried for 2h at 140 °C and then calcined in air at 400 °C for 5h with a heating rate of 10 °C/min to obtain Fe or Co silica aerogels. Before the experiments, the catalysts samples were reduced in an H_2/N_2 (5%/95%) flow at 600 °C for 10 h with a heating rate of 10 °C/min.

The micro GC was calibrated for each gaseous component using standard gas cylinders with a wide range of concentrations. Based on the measurements of the micro GC and the difference in temperature, pressure, and flow rate before and during each experiment, the conversion rate (x) of H_2 and CO can be calculated as follows:

$$x_{CH_4} = \frac{moles\ of\ CH_4\ comsumed}{moles\ of\ CH_4\ inlet} \times 100\ \% \tag{1}$$

$$x_{CO_2} = \frac{moles\ of\ CO_2\ comsumed}{moles\ of\ CO_2\ inlet} \times 100\ \% \tag{2}$$

The selectivity and yield of gaseous products can be calculated as:

$$S_{H_2} = \frac{moles\ of\ H_2\ produced}{2 \times moles\ of\ CH_4\ consumed} \times 100\ \% \tag{3}$$

$$S_{CO} = \frac{moles\ of\ CO\ produced}{moles\ of\ CO_2\ consumed + moles\ of\ CH_4\ consumed} \times 100\ \% \tag{4}$$

$$Y_{H_2} = \frac{moles\ of\ H_2\ produced}{2 \times moles\ of\ CH_4\ input} \times 100\ \% \tag{5}$$

$$Y_{CO} = \frac{moles\ of\ CO\ produced}{moles\ of\ CO_2\ input + moles\ of\ CH_4\ input} \times 100\ \% \tag{6}$$

$$S_{C_xH_y} = \frac{x \times moles\ of\ C_xH_y\ produced}{moles\ of\ CO_2\ consumed + moles\ of\ CH_4\ consumed} \times 100\ \% \tag{7}$$

The selectivity of CH_4 to CO is defined as:

$$S_{CH_4/CO} = \frac{moles\ of\ CO\ produced - moles\ of\ CO_2\ consumed}{moles\ of\ CH_4\ consumed} \times 100\ \% \tag{8}$$

The ratio of unsaturated hydrocarbons/saturated hydrocarbons can be calculated as:

$$R = \frac{moles\ of\ unsaturated\ C_{2-5}}{moles\ of\ saturated\ C_{2-5}} \times 100\ \% \tag{9}$$

The carbon balance based on the inlet and outlet gas can be calculated as:

$$CB = \frac{moles\ of\ C\ outlet}{moles\ of\ C\ inlet} \times 100\ \% \tag{10}$$

The GCMS was calibrated using a standard liquid sample (20 vol% of methanol, ethanol, acetic acid, acetone, and water) to quantify the main products, and the results were normalized by abstracting water. As the selectivity to deposition was negligible as elaborated in supporting document, the selectivity towards liquid organics can then be calculated due to:

$$S_{liquid} = 100\% - S_{CO} - S_{C_xH_y} \tag{11}$$

$$S_{C_xH_yO_z} = x * mole\%\ of\ C_xH_yO_z\ *\ S_{liquid} \tag{12}$$

The specific input energy (SIE) is defined as the formula following:

$$SIE = \frac{Power\ of\ discharge(kW)}{Flow\ rate(\frac{L}{min})} * 60(\frac{s}{min}) \tag{13}$$

The energy efficiency (EE) of the reactor based on the gas conversion is defined as the reactants converted per unit of applied power:

$$E_{CO_2} = \frac{moles\ of\ CO_2\ consumed}{power} \tag{14}$$

$$E_{CH_4} = \frac{moles\ of\ CH_4\ consumed}{power} \tag{15}$$

3. Results and discussion

3.1. Plasma experiments without catalysts

The plasma experiments without catalysts were conducted using a variable CO_2/CH_4 ratio at a total flow rate of 30 mL/min and a variable total flow rate with a fixed CO_2/CH_4 ratio of 2:1. The temperature of the reactor obtained from the IR camera in all of the tests was around 55°C-65°C (Figure S4 of the supporting materials), which is far lower than the essential temperature to initiate the reaction of CO_2 and CH_4 according to the thermodynamic equilibrium calculation (Figure S1, S2 and S3 of the supporting materials). Hence, we consider that conventional thermochemical reactions did not contribute to the conversion of CO_2 and CH_4 [25]. The selectivity of gaseous products, conversion rate, and corresponding SIE are illustrated in Figure 1. Table 1 shows the applied power, selectivity of CH_4 to CO, and energy efficiency. CO, H_2, and C2-5 hydrocarbons, mostly alkanes, were synthesized as the major products. Methanol, acetic acid, some other oxygenates and a significant peak of water were also detected in the liquid composition; however, the total selectivity towards liquid organics was only around 0.1 or even less (the detailed composition of selectivity towards liquid products is not listed). It should be noted that the water was one part generated through the reactions; the other part was condensed from the air when opening the condensing bottle due to the temperature difference. In addition, a very small amount of carbon deposit was found on the surface of the reactor and electrode in some of the plasma experiments without catalysts, while only negligible carbon deposit was found after placing the aerogel catalysts. The CO_2/CH_4 ratio significantly affected the conversion rate of the reactants and the distribution of the products. The CO_2 and CH_4 conversion rates (from 19.2% and 37.8% to 29.6% and 43.2%) and the selectivity towards CO and H_2 (from 49% and 39.3% to 75.7% and 50.8%) increased with the CO_2/CH_4 ratio with almost the same SIE, while the selectivity towards C2-C5 hydrocarbons dramatically decreased (from 41.5% to 22.2%). The reactive species of CO_2 and CH_4 plasma, including CO, CO_2^+, O, OH, and CH_3, have been reported by some researchers [25, 30]. The initial steps for the electron-impact dissociation of CH_4 and CO_2 in a non-thermal plasma could be described as:

$$CO_2 + e \rightarrow CO + O + e \tag{16}$$

$$CH_4 + e \rightarrow CH_3 + H + e \tag{17}$$

$$CH_4 + e \rightarrow CH_2 + H_2 + e \tag{18}$$

$$CH_4 + e \rightarrow CH + H_2 + H + e \tag{19}$$

Simulation work on plasma methane conversion has revealed that reaction (17) is responsible for 79% of CH_4 dissociation, while reactions (18) and (19) contribute 15% and 5% respectively [36]. This indicates that one part of the generated H finally formed H_2 due to the selectivity towards H_2 shown in Figure 1, while another part of H may combine with O, leading to the formation of H_2O or OH species. The recombination reactions of CH_x with the subsequent radicals resulted in the formation of higher hydrocarbons and oxygenates. Increasing the CH_4 ratio indeed increased the reactive CH_3 radicals. Therefore, the selectivity towards C2-C5 alkanes significantly increased. It is notable that the ratio of unsaturated hydrocarbons to saturated hydrocarbons is negligible as shown in Table 1, indicating that the recombination reaction of H with unsaturated species was dominant in NTPs. Except for reaction (16), the vibrationally excited $CO_2(v)$ can also be generated in NTPs, and O radicals and H radicals can efficiently attack $CO_2(v)$ molecules to produce CO [5]:

$$CO_2(v) + O \rightarrow CO + O_2 \tag{20}$$

$$CO_2(v) + H \rightarrow CO + OH \tag{21}$$

However, recent simulation work [37] has demonstrated that the population of vibrational levels could be limited in DBD plasma, and the dominant CO_2-splitting mechanisms were direct electron impact dissociation. Based on this understanding, instead of attacking CO_2(v) molecules, the highly active O radicals could mainly combine with H to produce OH radicals and attack CH_4 molecules, along with producing OH and CH_3 radicals in the DBD reactor. Subsequently, the OH radicals could contribute to the formation of oxygenates (methanol, acetic acid, etc.) and water. Thus, O radicals could play a vital role in DBD plasma conversion of CO_2 with CH_4, and this explains the increase in the conversion rate, energy efficiency of both reactants, yield of syngas products with the increase of CO_2 ratio, and the higher conversion rate of CH_4 compared to CO_2. Another evidence was that no O_2 components were detected in the outlet gas, even with the highest CO_2 ratio, due to the limitation of reaction (20). We also noticed that the increase in CO_2 ratio increased the selectivity of CH_4 to CO. CH_3OH and CH_2O radicals are known to be easily decomposed when the translational temperature increases [5]. Therefore, the CH_xO radicals, which were generated via the recombination of O or OH with CH_x and contributed to the formation of oxygenates and chain growth, can also finally decompose into CO, H_2, and H_2O, resulting in the production of syngas instead of liquid organics. The increase in the CO_2 ratio certainly increased the CH_xO radicals, leading to more decomposition into CO. Regarding the low selectivity towards liquid organics, the reaction route of decomposition could be dominant in the gas phase in DBD plasma:

$$CH_x \xrightarrow{O,OH} CH_xO \xrightarrow{OH,H,O} CO, H_2, H_2O \qquad (22)$$

Increasing total flow rate will certainly reduce the residence time of reactants in the discharge area of the reactor, resulting in reducing the chance of reactant molecule to collide with electrons that had enough energy to for dissociation, leading to the decrease of discharge power at a certain input signal and the decrease of conversions. Meanwhile, the selectivity of CH_4 to CO_2 also reduced. The reasons could be the decrease in residence time and the lower translational temperature, which leads to less decomposition of oxygenated radicals and high total selectivity of liquid organics.

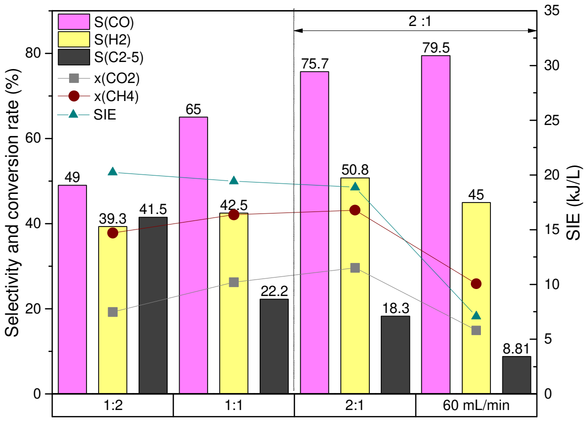

Figure 1. The selectivity of gaseous products, the conversion rates of reactants and the corresponding SIE varied by CO_2/CH_4 ratio and total flow rate without catalysts (peak-to-peak voltage: 5.5 kV, frequency: 3 kHz).

Table 1. Applied power, the selectivity of CH_4 to CO, carbon balance, and the energy efficiency of the plasma experiments varied by CO_2/CH_4 ratio and total flow rate without catalysts (peak-to-peak voltage: 5.5 kV, frequency: 3 kHz).

	$S_{CH4\ to\ CO}$	R	Power (W)	EE (mmol/kJ)		Yield (%)		CB
				CO_2	CH_4	CO	H_2	
1:2	0.357	0.051	10.1	0.129	0.508	15.44	14.85	0.983
1:1	0.414	0.037	9.71	0.276	0.442	22.00	17.87	0.966
2:1	0.513	0.033	9.45	0.427	0.311	26.57	21.91	0.984
60 mL/min	0.392	0.022	7.08	0.573	0.497	11.64	13.43	0.973

The plasma experiments with only CH_4 or CO_2 were also carried out without catalysts at the same peak-to-peak voltage, frequency, and total flow rate (30mL/min). As shown in Figure 2, the conversion rates of CH_4 only (28.6%) and CO_2 only (15.2%) experiments are much lower than those of the gas mixture. Considering that the recombination of O_2 and CO occurred in NTP conditions, it is reasonable that the conversion is lower than the tests of the gas mixture, in which the O mainly reacted with CH_x and H radicals as mentioned above. As a result, the conversion of CH_4 seemed to be greatly promoted by O, while the conversion of CO_2 was relatively less promoted by H according to reaction (21), and the recombination of O_2 and CO was inhibited. The results confirmed that O was vital to the conversion of CH_4. However, O_2, as the main product of dissociation of CO_2, was not found in the CO_2/CH_4 plasma due to the activity of O_2 and the limitation of reaction (20). We also found that the carbon balance of the CO_2-only test was almost 100%, while with CH_4 only the carbon balance was around 95%. In fact, the threshold energy for the electron impact dissociation of CH_4 into carbon black (~14 eV) is much higher than the average electron energy of DBD, thus inhibiting the formation of carbon deposition. This indicated that CH_4 mainly attributed to the tiny amount of carbon black. Based on this analysis, the possible reaction pathway under these conditions is proposed as shown in Scheme 3.

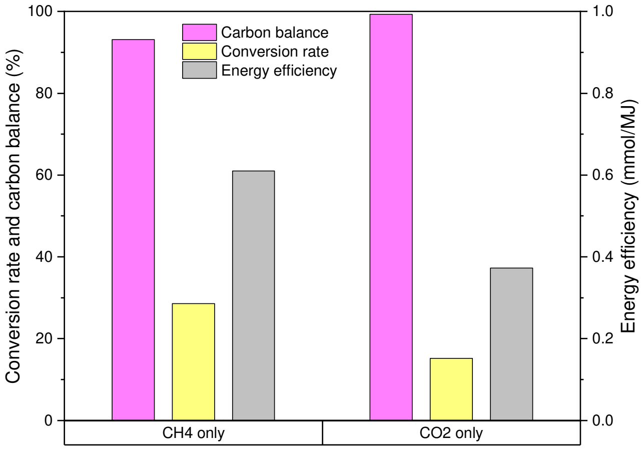

Figure 2. The carbon balance, conversion rates, and energy efficiency of CH_4-only or CO_2-only conditions without catalysts (peak-to-peak voltage: 5.5 kV, frequency: 3 kHz).

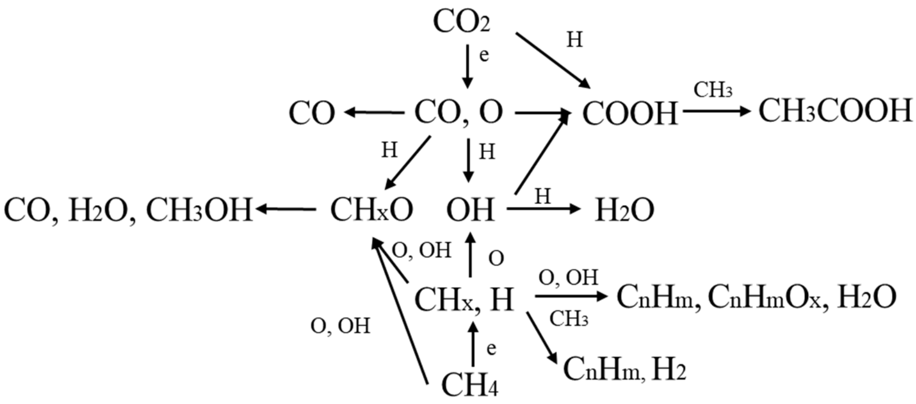

Scheme 3. Possible reaction pathways for the formation of gaseous and liquid products

3.2 Plasma experiments with catalysts

The plasma-catalytic experiments were carried out with reduced Co/SiO_2 aerogel and Fe/SiO_2 aerogel catalysts using a total flow rate of 30 mL/min, the same input electrical signal, and a variable CO_2/CH_4 ratio. Figures 3 and 4 show the conversion rates, SIE, and energy efficiency without/with packing using a CO_2/CH_4 ratio of 2:1

respectively; Figures 5 and 6 illustrate the corresponding selectivity of gaseous products and main liquid products respectively. As the selectivity towards liquid products is almost negligible compared to the experiments with packing, only the results with packing are listed. The total selectivity towards liquid without packing is shown in Table 1. Methanol, ethanol and acetic acid were detected as the main liquid products, while a small amount of acetone, 1-propanol, and methyl acetate was also found with the Co and Fe catalysts. Compared to no-packing conditions, introducing the SiO_2 aerogel support negligibly altered the conversion rates and the energy efficiency of CO_2 and CH_4, while the selectivity towards methanol increased. Unlike Al_2O_3 support [24], fully packing the SiO_2 aerogel support did not significantly alter the discharge behavior and decrease the conversions (Figure S5 of supporting materials). The reason could be the high sorption capacity of SiO_2 aerogel, which caused the sorption of reactive species, such as CH_xO, into the mesoporous structure of silica aerogel (Table S1 of supporting materials), whereas previous simulation work [38] demonstrated that plasma was hardly formed. As a result, the decomposition of CH_xO into CO could be inhibited, and the residence time could also increase, thus decreasing the selectivity of CH_4 to CO (from 0.513 to 0.369) and promoting the formation of liquid organics. We can also observe a difference between the SiO_2 aerogel support before and after the experiments (Figure S6 of the supporting materials). For further characterization of the deposition on the aerogels, which lead to the color change, TGA and XPS tests were conducted on the spent SiO_2 sample as shown in Figure S11, S12, and S13. It was found carbon-containing deposits including carbon deposition and carbon-containing polymers or monomers were formed on the surface of spent SiO_2 sample rather than only carbon black (Figure S12 and S13). Moreover, it was found that the overall selectivity towards carbon-containing deposits was less than 3% according to the TGA analysis (Figure S11). Therefore, it was not considered when calculating the selectivity to liquid products.

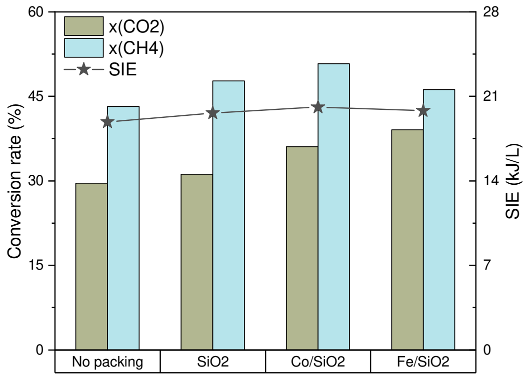

Figure 3. The conversion rates and SIE of the experiments without packing, with SiO_2 only, and with catalysts (peak-to-peak voltage: 5.5 kV, frequency: 3 kHz, total flow rate: 30 mL/min, CO_2/CH_4 ratio = 2:1).

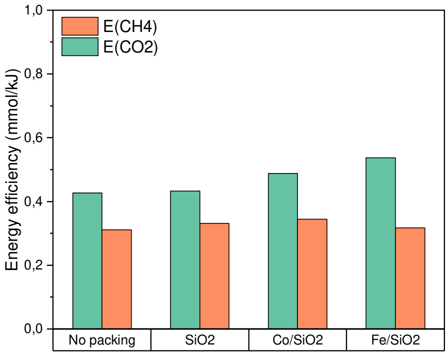

Figure 4. The energy efficiency of CO_2 and CH_4 without packing, with SiO_2 only, and with catalysts (peak-to-peak voltage: 5.5 kV, frequency: 3 kHz, total flow rate: 30 mL/min, CO_2/CH_4 ratio = 2:1).

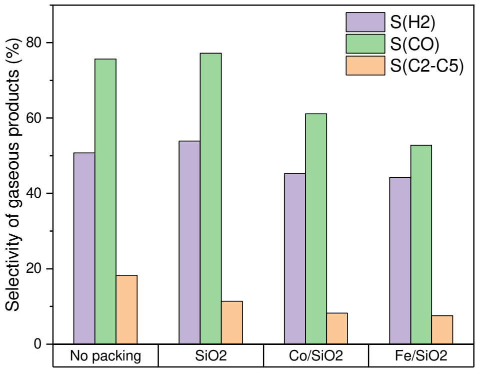

Figure 5. The selectivity of gaseous products without packing, with SiO_2 only, and with catalysts (peak-to-peak voltage: 5.5 kV, frequency: 3 kHz, total flow rate: 30 mL/min, CO_2/CH_4 ratio = 2:1).

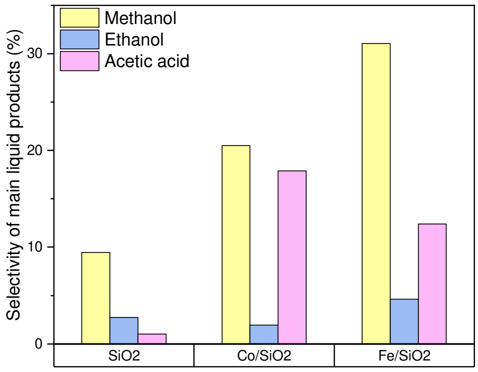

Figure 6. The selectivity of main liquid products without packing, with SiO_2 only, and with catalysts (peak-to-peak voltage: 5.5 kV, frequency: 3 kHz, total flow rate: 30 mL/min, CO_2/CH_4 ratio = 2:1).

Introducing the Co or Fe catalyst with its SiO_2 aerogel support greatly promoted the formation of liquid organics compared to SiO_2 aerogel only or no packing, as shown in Figure 6. Moreover, the conversion rates and energy efficiency of CO_2 and CH_4 increased, while the selectivity towards gaseous products significantly decreased. We also noted that the Co and Fe catalyst exhibited effects on discharge behavior (Figure S4) due to an abatement of discharge volume and the modification of conductivity, resulting in a slight increase in discharge power. In addition to the mesoporous structure of the SiO_2 aerogel, the well-dispersed Co and Fe in the supports significantly affected the selectivity of the products and shifted them towards liquid organics (methanol up to 20.5% and 31.0%, acetic acid up to 17.9% and 12.4%). The synergistic effects between catalysts and plasma are quite complicated and debated. Possible explanations are: 1) the introduction of the catalysts altered the discharge behavior, leading to the transition to more stable surface discharge as shown in Figure S5 [39]; 2) the strong sorption behavior of the mesoporous structure in the support, as mentioned above, inhibited the decomposition of CH_xO species; 3) the well-dispersed Co and Fe, two conventional catalysts used for the direct synthesis of long-chain products in conventional FTS and CO_2 hydrogenation process, remarkably enhanced the conversion of CO_2 and the formation of methanol and acetic acid. We also noted that Fe/SiO_2 was more favorable to alcoholic products with higher CO_2 conversion rates, while Co/SiO_2 favored the formation of acetic acid with a higher conversion rate of CH_4 when comparing the distribution of products between the two catalysts. Furthermore, more long-chain chemicals (propanol, methyl acetate) were detected in the liquid products via GC-MS with packing Co/SiO_2 than packing Fe/SiO_2. One possible explanation is that Co, as a widely used catalyst for chain growth in conventional FTS process, could be more capable of activating CH_4 into CH_x and thus naturally more active in chain propagation. Meanwhile, Fe, which is well known to be capable of activating CO_2 in CO_2 hydrogenation process, could lead to more enrichment of OH radicals, which ultimately contribute to the formation of short-chain alcohols at low temperatures. For the characterization and comparison of deposition on Co/SiO_2 and Fe/SiO_2, the C1s XPS spectra of catalyst samples and SiO_2 were normalized to compare the intensity as shown in Figure S14. The results indicated that the carbon-containing deposits were even much less formed on the Co/SiO_2 and Fe/SiO_2 samples than on the SiO_2 sample. Moreover, the peaking results of the corresponding C1s peaks (Figure S15) revealed that more organic deposition (polymer or monomer) rather than carbon deposition were formed on these catalyst samples.

Plasma-catalytic experiments with various CO_2/CH_4 ratios were also conducted under the same conditions. The selective tendency of gaseous products that vary by CO_2/CH_4 ratio with packing catalysts is similar to the results without packing catalysts as shown in Figure 8. Decreasing the CO_2/CH_4 ratio logically leads to the generation of CH_3 radicals, therefore promoting the formation of long-chain products, such as ethanol, and decreasing the selectivity towards methanol. Indeed, more long-chain oxygenated species were detected, and hydrocarbons with particularly long chains (hexane, heptane) were found in the liquid products with the Co/SiO_2 catalyst (Figure S7 of supporting materials). Note that decreasing the CO_2/CH_4 ratio significantly increased the selectivity towards acetic acid. As shown in Scheme 3, COOH radicals could be formed via the recombination of CO radicals with OH radicals and the combination of CO_2 and H radicals. Thus the selectivity towards acetic acid should logically decrease because fewer CO radicals and O radicals were generated in this condition. The results suggest that the catalysts could promote the conversion of CO_2 into COOH radicals instead of CH_xO, and that production could depend more on H radicals than on CO_2. It was clearly established once more that, whatever the ratio of CO_2/CH_4, the Co catalyst was more sensitive to acetic acid and long-chain products, while the Fe catalyst was more favorable to alcoholic products. Based on these results, we suggest that both Co and Fe are capable of activating the reactants and active to adsorb the radicals, especially O, OH, and CH_x produced in NTP. Meanwhile, the adsorbed CH_x can efficiently react with the adjacent OH to produce CH_xO and alcoholic products, mainly methanol. The adsorbed CO_2 could react with the H radicals in the gas phase to produce COOH radicals, leading to the formation of organic acids, mainly acetic acid; the adsorbed CH_x and CH_xO would combine to form long-chain oxygenates (propanoic acid, butanol, etc.), or even react with H in the gas phase to produce long hydrocarbons and water, which in our study was responsible for the chain growth. Following this assumption, a possible pathway is proposed in Scheme 4. Significant results detected a small amount of hexane, heptane and C6 ester ($C_6H_{12}O_2$) in liquid products using a CO_2/CH_4 ratio of 2:1 with Co catalysts, while a small amount of pentanol and heptanol were found in the liquid products with Fe catalysts under the same conditions. Consequently, the direct synthesis of value-added liquid chemicals and syngas was achieved with interesting selectivity and energy efficiency via this plasma-catalytic process.

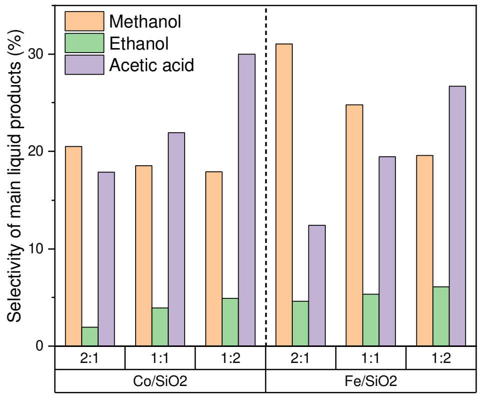

Figure 7. The selectivity of main liquid products as a function of catalysts and a CO_2/CH_4 ratio from 2:1 to 1:2 (peak-to-peak voltage: 5.5 kV, frequency: 3 kHz, total flow rate: 30 mL/min).

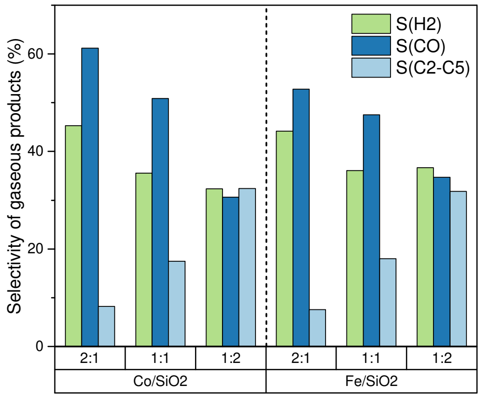

Figure 8. The selectivity of gaseous products as a function of catalysts and a CO_2/CH_4 ratio from 2:1 to 1:2 (peak-to-peak voltage: 5.5 kV, frequency: 3 kHz, total flow rate: 30 mL/min).

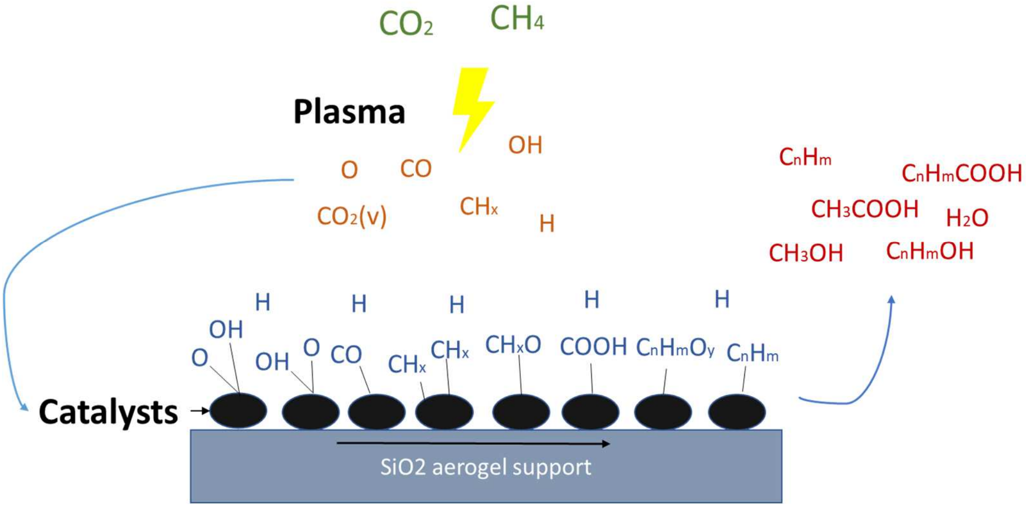

Scheme 4. Possible reaction pathways for the formation of liquid products on the catalysts via plasma-catalytic approach.

4. Conclusion

In this study, the direct synthesis of value-added liquid chemicals from CO_2 and CH_4 by a plasma-catalytic process was achieved with considerable conversion rates at ambient conditions. The influence of different CO_2/CH_4 ratios, SiO_2 aerogel packing, and supported catalysts packing was investigated.

Without packing, it was found that syngas and C2 to C5 gaseous hydrocarbons were the main products, while the total selectivity towards liquid products was negligible, mainly due to the decomposition of CH_xO radicals. Increasing the CO_2/CH_4 ratio increased the conversions of both reactants and the selectivity towards syngas, while selectivity towards C2+ species decreased.

With packing, the results were very different. Firstly, the use of aerogel as a support for the catalyst made it possible to avoid: (i) a significant abatement in discharge volume, (ii) an alteration of the discharge behavior. Moreover, due to its high sorption capacity, the packing version slightly favored the formation of liquid chemicals. Secondly, the synergetic addition of an appropriate catalyst in the system significantly promoted the formation of the liquid chemicals up to a total liquid selectivity of 40%, where methanol and acetic acid were the main liquid products. The results also revealed that the Fe catalyst preferentially led to the formation of alcoholic products, while a Co catalyst was more favorable to the formation of acids and long-chain products (up to C5 oxygenates). Moreover, with a high ratio of CH_4, a few C5+ hydrocarbons (pentane and heptane) and a C6 ester were synthesized. To our knowledge, the plasma-catalytic performance for liquid production obtained here is outstanding compared to existing studies and broadens the way to the design of an efficient plasma-catalytic process for direct conversion of CO_2 and CH_4 into liquid chemicals.

Conflict of interest

The authors declare no competing financial interest.

Acknowledgments

This research was carried out in the frame of the cooperative doctoral programs (ParisTech/CSC) supported by the China Scholarship Council (CSC). The authors warmly acknowledge CSC for their support.

Appendix A. Supporting materials

References

[1] J. Koornneef, A. Ramírez, W. Turkenburg, A. Faaij, The environmental impact and risk assessment of CO2 capture, transport and storage–An evaluation of the knowledge base, Progress in Energy and Combustion Science, 38 (2012) 62-86.
[2] M. Aresta, A. Dibenedetto, A. Angelini, Catalysis for the valorization of exhaust carbon: from CO2 to chemicals, materials, and fuels. Technological use of CO2, Chemical reviews, 114 (2013) 1709-1742.
[3] C.W. Li, J. Ciston, M.W. Kanan, Electroreduction of carbon monoxide to liquid fuel on oxide-derived nanocrystalline copper, Nature, 508 (2014) 504.
[4] Y.H. Hu, E. Ruckenstein, Catalytic conversion of methane to synthesis gas by partial oxidation and CO2 reforming, ChemInform, 35 (2004) no-no.
[5] A. Fridman, Plasma chemistry, Cambridge university press2008.
[6] Y. Yang, Methane conversion and reforming by nonthermal plasma on pins, Industrial & engineering chemistry research, 41 (2002) 5918-5926.
[7] N. Seyed-Matin, A.H. Jalili, M.H. Jenab, S.M. Zekordi, A. Afzali, C. Rasouli, A. Zamaniyan, DC-pulsed plasma for dry reforming of methane to synthesis gas, Plasma Chemistry and Plasma Processing, 30 (2010) 333-347.
[8] A. Aziznia, H.R. Bozorgzadeh, N. Seyed-Matin, M. Baghalha, A. Mohamadalizadeh, Comparison of dry reforming of methane in low temperature hybrid plasma-catalytic corona with thermal catalytic reactor over Ni/γ-Al 2 O 3, Journal of Natural Gas Chemistry, 21 (2012) 466-475.
[9] J. Sentek, K. Krawczyk, M. Młotek, M. Kalczewska, T. Kroker, T. Kolb, A. Schenk, K.-H. Gericke, K. Schmidt-Szałowski, Plasma-catalytic methane conversion with carbon dioxide in dielectric barrier discharges, Applied Catalysis B: Environmental, 94 (2010) 19-26.
[10] K.L. Pan, W.C. Chung, M.B. Chang, Dry reforming of CH 4 with CO 2 to generate syngas by combined plasma catalysis, IEEE Transactions on Plasma Science, 42 (2014) 3809-3818.
[11] W.-C. Chung, K.-L. Pan, H.-M. Lee, M.-B. Chang, Dry reforming of methane with dielectric barrier discharge and ferroelectric packed-bed reactors, Energy & Fuels, 28 (2014) 7621-7631.
[12] D. Li, X. Li, M. Bai, X. Tao, S. Shang, X. Dai, Y. Yin, CO 2 reforming of CH 4 by atmospheric pressure glow discharge plasma: a high conversion ability, International Journal of Hydrogen Energy, 34 (2009) 308-313.
[13] H. Long, S. Shang, X. Tao, Y. Yin, X. Dai, CO 2 reforming of CH 4 by combination of cold plasma jet and Ni/γ-Al 2 O 3 catalyst, international journal of hydrogen energy, 33 (2008) 5510-5515.
[14] L. Xiang, M.-g. BAI, X.-m. TAO, S.-y. SHANG, Y.-x. YIN, X.-y. DAI, Carbon dioxide reforming of methane to synthesis gas by an atmospheric pressure plasma jet, Journal of Fuel Chemistry and Technology, 38 (2010) 195-200.
[15] A. Indarto, J.-W. Choi, H. Lee, H.K. Song, Effect of additive gases on methane conversion using gliding arc discharge, Energy, 31 (2006) 2986-2995.
[16] Z. Bo, J. Yan, X. Li, Y. Chi, K. Cen, Plasma assisted dry methane reforming using gliding arc gas discharge: effect of feed gases proportion, International Journal of Hydrogen Energy, 33 (2008) 5545-5553.
[17] X. Tu, J.C. Whitehead, Plasma dry reforming of methane in an atmospheric pressure AC gliding arc discharge: co-generation of syngas and carbon nanomaterials, International Journal of Hydrogen Energy, 39 (2014) 9658-9669.

[18] K. Zhang, B. Eliasson, U. Kogelschatz, Direct conversion of greenhouse gases to synthesis gas and C4 hydrocarbons over zeolite HY promoted by a dielectric-barrier discharge, Industrial & engineering chemistry research, 41 (2002) 1462-1468.
[19] K. Zhang, U. Kogelschatz, B. Eliasson, Conversion of greenhouse gases to synthesis gas and higher hydrocarbons, Energy & fuels, 15 (2001) 395-402.
[20] T. Jiang, Y. Li, C.-j. Liu, G.-h. Xu, B. Eliasson, B. Xue, Plasma methane conversion using dielectric-barrier discharges with zeolite A, Catalysis Today, 72 (2002) 229-235.
[21] K. Zhang, T. Mukhriza, X. Liu, P.P. Greco, E. Chiremba, A study on CO2 and CH4 conversion to synthesis gas and higher hydrocarbons by the combination of catalysts and dielectric-barrier discharges, Applied Catalysis A: General, 502 (2015) 138-149.
[22] A.-J. Zhang, A.-M. Zhu, J. Guo, Y. Xu, C. Shi, Conversion of greenhouse gases into syngas via combined effects of discharge activation and catalysis, Chemical Engineering Journal, 156 (2010) 601-606.
[23] F. Zhu, H. Zhang, X. Yan, J. Yan, M. Ni, X. Li, X. Tu, Plasma-catalytic reforming of CO2-rich biogas over Ni/γ-Al2O3 catalysts in a rotating gliding arc reactor, Fuel, 199 (2017) 430-437.
[24] X. Tu, H.J. Gallon, M.V. Twigg, P.A. Gorry, J.C. Whitehead, Dry reforming of methane over a Ni/Al2O3 catalyst in a coaxial dielectric barrier discharge reactor, Journal of Physics D: Applied Physics, 44 (2011) 274007.
[25] X. Tu, J. Whitehead, Plasma-catalytic dry reforming of methane in an atmospheric dielectric barrier discharge: Understanding the synergistic effect at low temperature, Applied Catalysis B: Environmental, 125 (2012) 439-448.
[26] J.-J. Zou, Y.-p. Zhang, C.-J. Liu, Y. Li, B. Eliasson, Starch-enhanced synthesis of oxygenates from methane and carbon dioxide using dielectric-barrier discharges, Plasma Chemistry and Plasma Processing, 23 (2003) 69-82.
[27] M. Scapinello, L.M. Martini, P. Tosi, CO2 hydrogenation by CH4 in a dielectric barrier discharge: catalytic effects of nickel and copper, Plasma Processes and Polymers, 11 (2014) 624-628.
[28] V. Goujard, J.-M. Tatibouët, C. Batiot-Dupeyrat, Use of a non-thermal plasma for the production of synthesis gas from biogas, Applied Catalysis A: General, 353 (2009) 228-235.
[29] K. Kozlov, P. Michel, H.-E. Wagner, Synthesis of organic compounds from mixtures of methane with carbon dioxide in dielectric-barrier discharges at atmospheric pressure, Plasmas and Polymers, 5 (2000) 129-150.
[30] L. Wang, Y. Yi, C. Wu, H. Guo, X. Tu, One‐step reforming of CO2 and CH4 into high‐value liquid chemicals and fuels at room temperature by plasma‐driven catalysis, Angewandte Chemie International Edition, 56 (2017) 13679-13683.
[31] H. Takeda, H. Kamiyama, K. Okamoto, M. Irimajiri, T. Mizutani, K. Koike, A. Sekine, O. Ishitani, Highly Efficient and Robust Photocatalytic Systems for CO2 Reduction Consisting of a Cu(I) Photosensitizer and Mn(I) Catalysts, Journal of the American Chemical Society, 140 (2018) 17241-17254.
[32] X. Wang, X. Zhao, D. Zhang, G. Li, H. Li, Microwave irradiation induced UIO-66-NH2 anchored on graphene with high activity for photocatalytic reduction of CO2, Applied Catalysis B: Environmental, 228 (2018) 47-53.
[33] R. Yadav, V. Amoli, J. Singh, M.K. Tripathi, P. Bhanja, A. Bhaumik, A.K. Sinha, Plasmonic gold deposited on mesoporous TixSi1−xO2 with isolated silica in lattice: An excellent photocatalyst for photocatalytic conversion of CO2 into methanol under visible light irradiation, Journal of CO2 Utilization, 27 (2018) 11-21.

[34] S. Iwarere, V. Rohani, D. Ramjugernath, F. Fabry, L. Fulcheri, Hydrocarbons synthesis from syngas by very high pressure plasma, Chemical Engineering Journal, 241 (2014) 1-8.
[35] V. Rohani, S. Iwarere, F. Fabry, D. Mourard, E. Izquierdo, D. Ramjugernath, L. Fulcheri, Experimental study of hydrocarbons synthesis from syngas by a tip–tip electrical discharge at very high pressure, Plasma Chemistry and Plasma Processing, 31 (2011) 663.
[36] C. De Bie, B. Verheyde, T. Martens, J. van Dijk, S. Paulussen, A. Bogaerts, Fluid modeling of the conversion of methane into higher hydrocarbons in an atmospheric pressure dielectric barrier discharge, Plasma Processes and Polymers, 8 (2011) 1033-1058.
[37] T. Kozák, A. Bogaerts, Splitting of CO2 by vibrational excitation in non-equilibrium plasmas: a reaction kinetics model, Plasma Sources Science and Technology, 23 (2014) 045004.
[38] Y.R. Zhang, K. Van Laer, E.C. Neyts, A. Bogaerts, Can plasma be formed in catalyst pores? A modeling investigation, Appl. Catal. B-Environ., 185 (2016) 56-67.
[39] D. Mei, X. Zhu, Y.-L. He, J.D. Yan, X. Tu, Plasma-assisted conversion of CO2 in a dielectric barrier discharge reactor: understanding the effect of packing materials, Plasma Sources Science and Technology, 24 (2014) 015011.

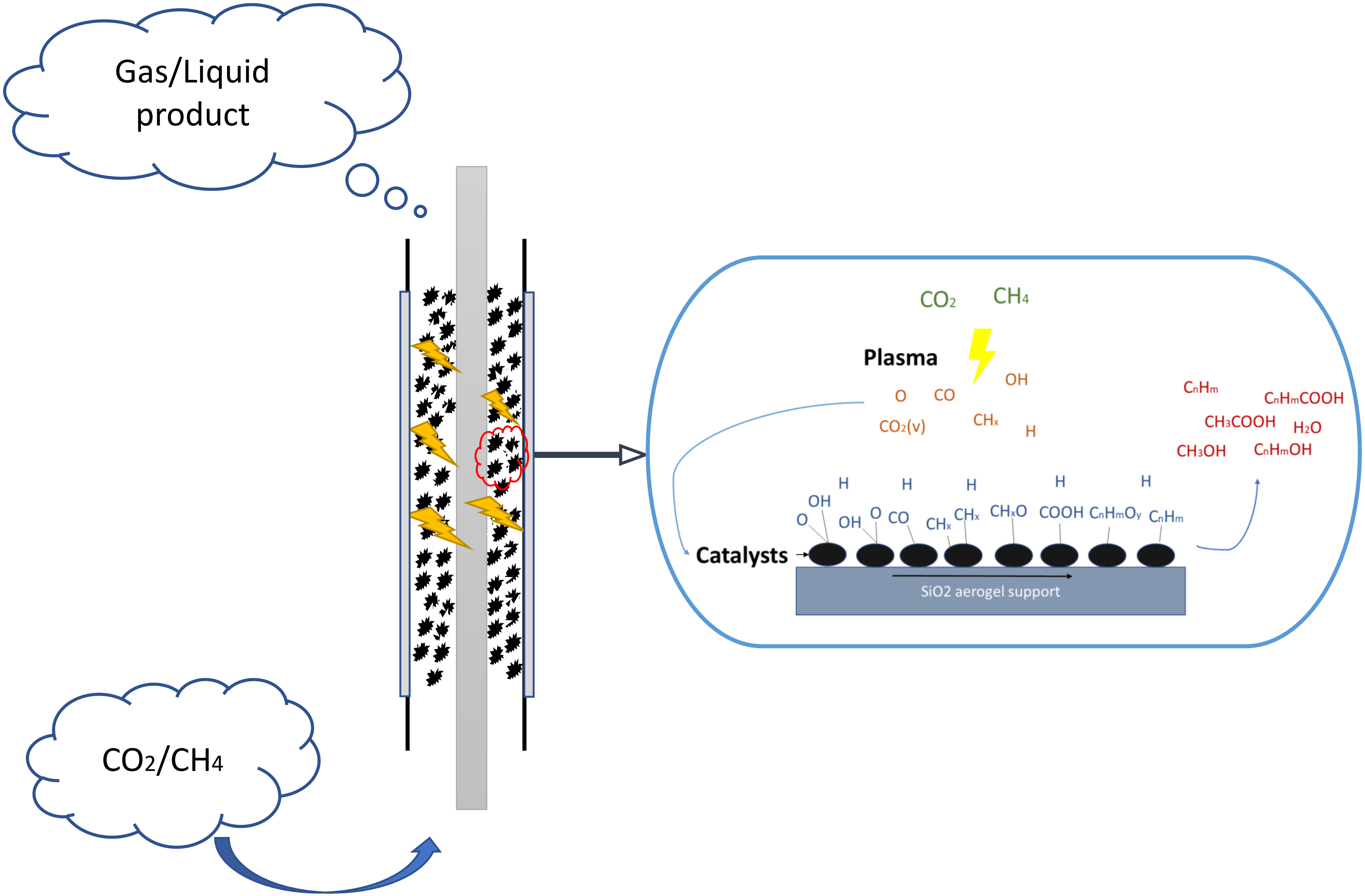
Gas/Liquid product
CO_2/CH_4
CO_2
CH_4
Plasma
OH
O
CO
CO_2(v)
CH_x
H
C_nH_m
C_nH_mCOOH
CH_3COOH
H_2O
CH_3OH
C_nH_mOH
H
H
H
H
H
OH
O
OH
O
CO
CH_x
CH_x
CH_xO
COOH
$C_nH_mO_y$
C_nH_m
Catalysts
SiO2 aerogel support